FLUVIAL REWORKING ELIMINATES SMALL CRATERS, BUT DOES NOT MEANINGFULLY BIAS THE MARS INTERBEDDED-CRATER RECORD. Andrew J. Moodie and Timothy A. Goudge, Jackson School of Geosciences, The University of Texas at Austin

Introduction: The accumulated history of crater production and destruction is recorded in crater size-frequency distributions (CSFDs), which can be leveraged to understand the evolution of planetary surfaces and atmospheres [1]. For example, Kite *et al.* [2] used the size-frequency distribution of craters interbedded with fluvial deposits to provide an upper-bound of $\sim$1.9 bar on paleo-atmospheric pressure at the time of river activity on Mars. Importantly, interpreting paleo-atmospheric pressure is sensitive to preservation and mapping of smaller craters ($\lesssim$50 m) [3], which is known to be influenced by a myriad of crater-destroying processes [4, 10] and image resolution effects [5].

River activity includes spatially and temporally heterogeneous deposition and erosion, which combine to create a stratigraphic record that is rife with gaps and bias in recorded time. This fluvial reworking is scaled by the channel depth [6], and coincidentally, typical channel depths have similar absolute scales to depths of smaller craters (channel and crater depths 10^0–10^1 m, for craters $\lesssim$50 m diameter). To approximate small-crater removal by sedimentary processes, Warren *et al.* [3] filtered CSFDs with an analytical size-dependent function, and found that sedimentary processes combined with higher paleo-atmopsheric pressure cannot reproduce the observed CSFDs, implying that interpreted pressure upper-bounds are robust. Despite the CSFD sourcing areas of reworked fluvial deposits, the filter's functional form has not been validated.

Excitingly, a well-calibrated crater removal function would enable paleo-atmospheric pressure upper-bounds to be translated into quantitative pressure estimates. In our study, we apply a forward model of coeval river-delta evolution and crater production, and then examine how CSFDs are impacted by fluvial reworking.

Methods: We simulated river-delta development [7] and coeval crater production via an imposed power-law CSFD [-2 exponent; 8] with crater diameters 5–250 m, and placed randomly and with a parameterized geometry [9] (Fig. 1). The imposed CSFD density corresponds to fluvial deposition lasting 4.5–6.5 Ma, although this is an easily varied model parameter. Crater production is instantaneous and has no effect on substrate erodibility in our model, and simulations neglect any additional processes that reduce crater mappability [e.g., 4, 10].

Landscape development over time generates stratigraphy that includes fluvial deposits and crater rim and ejecta material. We identified 560 interbedded craters across five replicate simulations, demarcated the rim annulus area (i.e., excluding the crater floor and ejecta material), and calculated the angle subtended by the largest contiguous segment of the rim remaining in the stratigraphy (i.e., a central arc angle; Fig. 2a). Including buried craters avoids post-depositional exhumation bias unevenly exposing larger buried crater rims [3, 11], so results reflect only fluvial reworking bias.

Finally, we made empirical crater diameter cumulative distribution functions (i.e., CSFDs) by applying thresholds to represent how crater mapping is affected by variable-resolution images and confidence in interpreting crater rim morphology. Craters smaller than 3$\times$ image resolution (dx) are not reliably mapped [10], which sets a crater counting threshold of $3\times dx = 3\times 10$ m $= 30$ m for the model results (orange CSFD in Fig. 2b); we also made CSFDs using a 0 m threshold (purple CSFD; i.e., no image resolution threshold) and a 10 m threshold (pink CSFD; approximately $3\times dx$ for images used in Kite *et al.* [2]). Kite *et al.* [2] asserted a minimum of 180° central arc angle of rim must be mappable to confidently count a crater; we applied a minimum preserved-rim central arc angle threshold when calculating CSFDs, using $\geq$180° as the primary distribution (solid colored lines in Fig. 2b), and $\geq$45° and $\geq$315° to assess distribution uncertainty (shaded colored area in Fig. 2b).

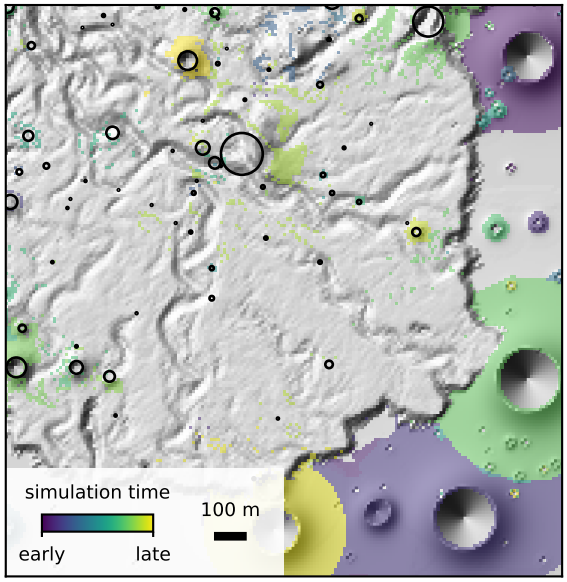

Figure 1: Topographic hillshade of coeval river-delta and crater production model, with crater rim and ejecta material at the surface colored by crater formation time. Black circles highlight interbedded crater rim locations. Area shown is $\sim$4 km^2 (half of the model domain).

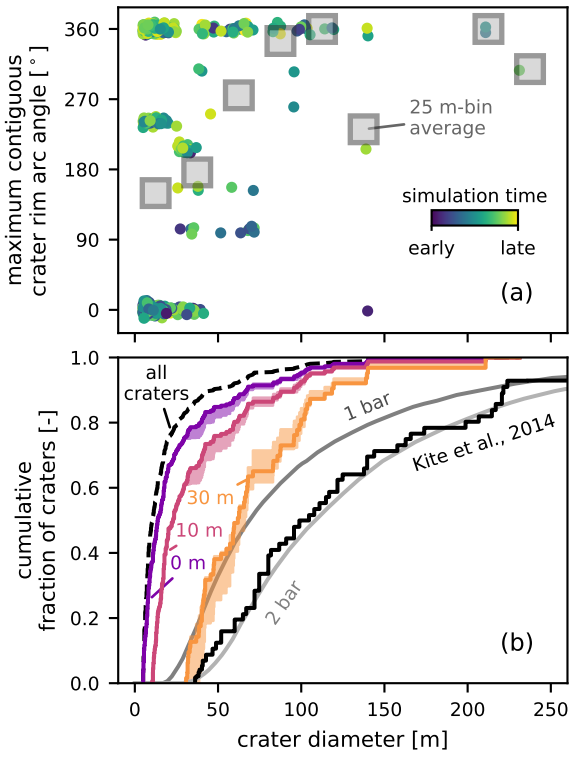

Figure 2: a) Maximum contiguous crater rim arc angle for interbedded craters ($\pm 1.5°$ and ± 1.5 m point jitter added for visualization), versus crater diameter, with gray boxes marking mutually exclusive 25 m-bin averages. b) Empirical CSFDs of all modeled craters (dashed black line), preserved and mappable craters (colors), and interbedded craters mapped by Kite *et al.* [2] (solid black line); results are compared to CSFDs predicted for paleo-atmospheric pressures (solid gray lines) [2]. For preserved and mappable CSFDs, an image resolution threshold excludes craters <0 m (purple; i.e., no resolution threshold), <10 m (pink), and <30 m, and an interpretability threshold excludes craters with central arc angle $<180°$ (solid line), and $<45°$ or $<315°$ (shaded area).

Results and discussion: We find that the maximum preserved-rim central arc angle varies from 0° to 360° (i.e., fully eroded to fully preserved) for craters $\lesssim$50 m, and that variability converges towards full preservation as crater diameter increases (Fig. 2a). Approximately 67% of craters $\lesssim$50 m have been at least partially eroded, with 53% of these craters having less than 180° of contiguous rim remaining. Notably, preservation does not depend on crater formation time. These results indicate that fluvial reworking can eliminate a substantial fraction of coevally produced craters (i.e., interbedded craters), especially biasing the smaller-crater record.

The CSFD of preserved and mappable craters is shifted from the CSFD of all modeled craters (purple and dashed black CSFDs, Fig. 2b). Although about half of the smaller craters ($\lesssim$50 m) are not mappable ($<180°$ central arc angle), there are so many smaller craters produced that the shift in CSFD is minor. The images used by Kite *et al.* [2] would have made reliably mapping craters $\lesssim$10 m difficult, and while the CSFD calculated using a 10 m image-resolution threshold (pink CSFD, Fig. 2b) is further shifted from the imposed CSFD, it also does not approach the Kite *et al.* [2] observed CSFD. The 30 m image-resolution filter (appropriate if modeled craters were to be mapped manually) significantly shifts the CSFD, implying that CSFDs generated without high-resolution images cannot reliably generate paleo-atmospheric pressure estimates.

Our findings bolster previous studies that assert fluvial reworking and image-resolution bias are secondary controls to atmospheric ablation on CSFDs, indicating that paleo-atmospheric pressure upper-bounds may be translated into estimates (with uncertainty). Discussion of some future work needed to determine the viability of this approach follows. Our simulations explore CSFD bias imparted under a specific condition of fluvial reworking relative to deposition duration, but increased fluvial reworking increases stratigraphic record bias [6], so further experiments are needed to determine whether plausibly higher reworking meaningfully impacts CSFDs. Oppositely, the fluvial reworking effect on CSFDs would be decreased if plausibly higher production rates for smaller craters were used [8, 5]. To translate upper-bound interpretations to estimates, we will also need to develop robust functions for post-depositional exhumation bias [3], and consider additional surface processes that can eliminate craters from the record [10].

References: **[1]** C. I. Fassett, *Journal of Geophysical Research: Planets* **121**, 1900–1926 (2016). **[2]** E. S. Kite, J.-P. Williams, A. Lucas, O. Aharonson, *Nature Geoscience* **7**, 335–339 (Apr. 2014). **[3]** A. O. Warren, E. S. Kite, J.-P. Williams, B. Horgan, *Journal of Geophysical Research: Planets* **124**, 2793–2818 (2019). **[4]** M. R. Smith, A. R. Gillespie, D. R. Montgomery, *Geophysical Research Letters* **35** (2008). **[5]** J.-P. Williams *et al.*, *Meteoritics & Planetary Science* **53**, 554–582 (2018). **[6]** K. M. Straub, C. R. Esposito, *Journal of Geophysical Research: Earth Surface* **118**, 625–637 (2013). **[7]** A. J. Moodie, J. Hariharan, E. Barefoot, P. Passalacqua, *Journal of Open Source Software* (2021). **[8]** W. K. Hartmann, *Icarus* **174**, 294–320 (2005). **[9]** A. D. Howard, *Geomorphology* **91**, 332–363 (2007). **[10]** J. E. Richardson, *Icarus* **204**, 697–715 (2009). **[11]** E. S. Kite, J. Sneed, D. P. Mayer, S. A. Wilson, *Geophysical Research Letters* **44**, 3991–3999 (2017).